Cascade Control System for Two Axes Gimbal System with Mass Unbalance

Maher Abdo[1], Ali Reza Toloei[2], Ahmad Reza Vali[3], and Mohammad Reza Arvan[4]

Abstract— the application of inertial stabilization system is to stabilize the sensor's line of sight toward a target by isolating the sensor from the disturbances induced by the operating environment. The aim of this paper is to present two axes gimbal system. The equations of gimbals motion are derived using Lagrange equation considering the base angular motion and mass unbalance. The stabilization loop is constructed by identifying its components, then the traditional and cascade loops are defined. The overall control system is built using the cross coupling unit and simulated in MATLAB for the traditional and cascade control loops. A comparison study is carried out to investigate the gimbal system performance under different operational conditions. The simulation results prove the efficiency of the proposed cascade control which offers a better response than the traditional one, and improves further the transient and the steady-state response.

Index Terms— DC motor, Gimbal system, Inertial stabilization system, Inertial cross coupling, Line of sight, Rate gyro, Stabilization loop

1 INTRODUCTION

The optical equipments (such as IR, radar, laser, and television) have found a wide use in many important applications, for example image processing, guided missiles, tracking systems, and navigation systems. In such systems, the optical sensor axis must be accurately pointed from a movable base to a fixed or moving target. Therefore, the sensor's line of sight (LOS) must be strictly controlled. In such an environment where the equipment is typically mounted on a movable platform, maintaining sensor orientation toward a target is a serious challenge.

An Inertial Stabilization Platform (ISP) is an appropriate way that can solve this challenge [1]. Usually, two axes gimbal system is used to provide stabilization to the sensor while different disturbances affect it. The most important disturbance sources are the base angular motion, the dynamics of gimballed system, and the gimbal mass unbalance. It is therefore necessary to capture all the dynamics of the plant and express the plant in analytical form before the design of gimbal assembly is taken up [2]. The performance of a system depends heavily on the accuracy of plant modelling. A typical plant for such problems consists of an electro-mechanical gimbal assembly having angular freedom in one, two or three axes and one or more EO sensors [3].

The control of such LOS inertia stabilization systems is not a simple problem because of cross-couplings between the different channels. In addition, such systems are usually required to maintain stable operation and guarantee accurate pointing and tracking for the target even when there are changes in the system dynamics and operational conditions.

The mathematical model and the control system of two axes gimbal system have been studied in many researches. Concerning the mathematical model, several derivations have been proposed using different assumptions. In [4], the kinematics and geometrical coupling relationships for two degree of freedom gimbal assembly have been obtained for a simplified case when each gimbal is balanced and the gimballed elements bodies are suspended about principal axes.

[5] presented the equations of motion for the two axes gimbal configuration, based on the assumption that the gimbals are rigid bodies and have no mass unbalance. In [5], Extrand has shown that inertia disturbances can be eliminated by certain inertia symmetry conditions, and certain choices of inertia parameters can eliminate the inertia cross couplings between the channels of gimbal system. Both researches [4] and [5] mentioned above have not been simulated. A single degree of freedom (SDOF) gimbal operating in a complex vibration environment has been presented by Daniel in [6]. It has been illustrated how the vibrations excite both static and dynamic unbalance disturbance torques, which can be eliminated by statically and dynamically balancing the gimbal, which is regarded costly and time consuming [6].

In [7], the motion equations have been derived on the assumption that gimbals have no dynamic mass imbalance, and the mass distribution of gimbals is symmetrical with respect to the frame axes considered. In addition, the effects of base angular velocities were not highlighted. In [8], a two axes gimbal mechanism was introduced and just the modelling of azimuth axis was focused, the elevation angle was kept fixed and cross moments of inertia were taken to be zero. In both [5] and [9], the dynamical model of elevation and azimuth gimbals have been derived on the assumption that gimbals mass distribution is symmetrical with respect to the gimbals frame axes. Therefore, the products of inertia were neglected, and the model was simplified. It must be mentioned, that most of these researches considered that the elevation and azimuth channels are identical so that one axis was simulated and tested. Therefore, the cross coupling, which is caused by base angular motion and the properties of gimbal system dynamics, was ignored. Also, it was supposed that gimbals mass distribution is symmetrical so the gimbals have not dynamic unbalance. In addition, Newton' law has been utilized to derive the mathematical model.

1 *Corresponding author, Electrical Eng-Malek Ashter Uiniversity of Technology-Tehran, Email: maherabdo74@yahoo.com*
2 *Aerospace Dep-Shahid Beheshti Uiniversity-Tehran, Email: ToLoei@yahoo.com*
3 *Electrical Eng-Malek Ashter Uiniversity of Technology-Tehran, Email: ar.vali@aut.ac.ir*
4 *Electrical Eng-Malek Ashter University of Technology-Tehran, Emai: m_r_arvan@yahoo.com*

On the other hand, the control system of two axes gimbal configuration has been constructed using different control approaches. In [7], a proxy-based sliding mode has been applied on two axes gimbal system; also [10] proposed the sliding mode control under the assumption of uncoupled identical elevation and azimuth channels. In [11], modern synthesis tools such as linear quadratic regulator (LQR) or linear quadratic Gaussian with loop transfer recovery (LQG/LTR) control for a wideband controller have also been used in the line of sight stabilization for mobile land vehicle. Also, [12] presented a linear quadratic Gaussian (LQG) algorithm for estimating and compensating in real time a particular class of disturbances.

Besides conventional control methods mentioned above, some advance control techniques, such as fuzzy logical control (FLC) [13], robust control [14], variable structure control (VSC) [15], were also applied in LOS inertia stabilization systems during recent years. Also, the H∞ control methodology was used in [16] to design a high performance controller so as to control the rate of the line of sight. [17] Introduced an efficient full-matrix fuzzy logic controller for a gyro mirror line-of-sight stabilization platform. While a majority of these algorithms were complex and difficult to be realized, the conventional PID and its constructors are still the most used approach due to their simple structure, cheap costs, simple design and high performance [18].

In this paper, the two axes gimbal system is introduced. The gimbal system mathematical model is derived using Lgrange equation by considering the base angular motions, dynamics of gimballed system, and both static and dynamic gimbal mass unbalance. Also, the cascade control technique using PI controllers is introduced because of several practical advantages [19]. The well-known PI or more precisely the "Cascade PI" control is very attractive in terms of simplicity and popularity.

The control aims are mainly to achieve good transient and steady-state performance against the change of base angular velocity, the change of base acceleration, and the gimbal mass unbalance. The paper is organized in the following manner. In section 2, the problem is formulated then the equations of gimbals motion are derived in section 3. Afterwards, the concept of gimbal mass unbalance is highlighted in section 4. The traditional and cascade stabilization loops are investigated and constructed in section 5. Then, in section 6, the simulink model of two axes gimbal system is introduced and tested for variable base rates and accelerations. Finally, the conclusion remarks are highlighted in section 7. The full mathematical model derivation is illustrated in Appendices A, B.

2 Problem Formulation

The stabilization is usually provided to the sensor by suspending it on the inner gimbal of two axes gimbal system, as shown in Fig.1. Also, a rate gyro located on the inner gimbal is utilized to measure the angular rates in the two planes of interest. The gyro outputs are used as feedback to torque motors, related to the gimbals, to provide boresight error tracking and stabilization against angular base motion.

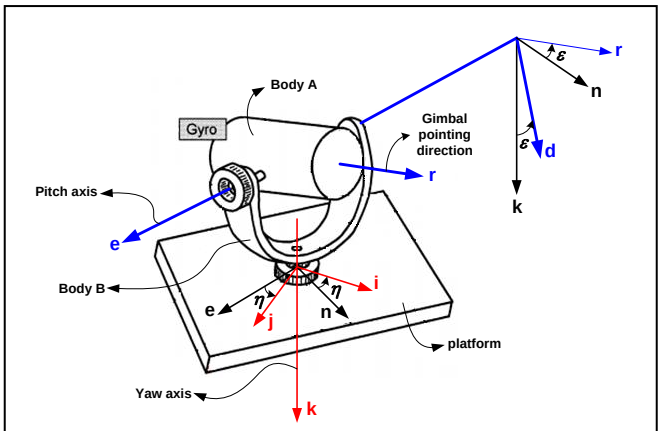

Fig. 1. Two axes gimbal system [20].

The overall control system is constructed utilizing two identical stabilization loops shown in Fig.2 for the inner (elevation) and outer (azimuth) gimbals.

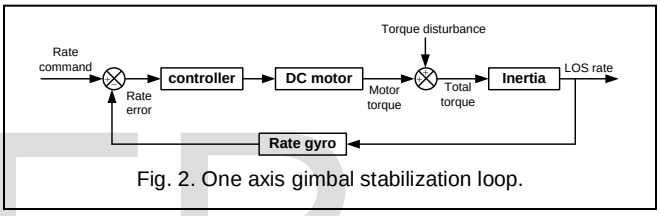

Fig. 2. One axis gimbal stabilization loop.

This system aims to isolate the stabilized object (sensor) from the base rotation. Therefore, the inner gimbal angular velocities, which are the outputs of the control system, must be made zero. In other words, the sensor optical axis must be kept nonrotating in an inertial space despite torque disturbances. The two control loops in elevation and azimuth channels are related to each other by the cross coupling unit which is built based on the relationships of torques affected on the two gimbals. The cross coupling express the properties of the gimbal system dynamics. It reflects the fact that the azimuth gimbal can affect on the elevation gimbal even when base body is nonrotating. Also, there is similar impact from the elevation gimbal on the azimuth gimbal. As a result, the cross coupling may be defined as the effect on one axis by the rotation of another [6].

The mass unbalance is a serious and inevitable imperfection that is encountred even in a well-designed gimbal system. The mass unbalance can cause disturbance torques on the gimbals when the base body is accelerating and rotating. Actually, to control a gimbal system and to provide stability to the sensor is a difficult task and it becomes more difficult especially when the gimbal system is utilized under variable operational conditions such as accelerations and angular velocities. In such operation environment, the drawback of the traditional stabilization loop shown in Fig.2 appears. Therefore, a cascade stabilization loop is suggested to solve this problem and guarantee high gimbal system performance according to desired requirements.

3 EQUATIONS OF GIMBALS MOTION

In this paper a two axes gimbal system depicted in Fig.1 is considered. Three reference frames are identified as follows. Frame P fixed to the fuselage body with axes (i, j, k), frame B fixed to the azimuth (outer) gimbal with axes (n, e, k), and frame A fixed to the elevation (inner) gimbal with axes (r, e, d). The r-axis coincides with the sensor optical axis. The k axis is pointing "downwards". The center of rotation is at the frame origin, which is assumed to be the same point for the three frames. The transformation matrices are obtained based on angles of rotation ε, η as follows

$$ {}^{B}_{P}C = \begin{bmatrix} \cos\eta & \sin\eta & 0 \\ -\sin\eta & \cos\eta & 0 \\ 0 & 0 & 1 \end{bmatrix}, \; {}^{A}_{B}C = \begin{bmatrix} \cos\varepsilon & 0 & -\sin\varepsilon \\ 0 & 1 & 0 \\ \sin\varepsilon & 0 & \cos\varepsilon \end{bmatrix} \quad (1) $$

Where ${}^{B}_{P}C$ is the transformation from frame P to frame B. Similarly, ${}^{A}_{P}C$ is the transformation from frame B to frame A. The inertial angular velocity vectors of frames P, B, and A, respectively are

$$ {}^{p}\bar{\omega}_{P/I} = \begin{bmatrix} \omega_{pi} \\ \omega_{pj} \\ \omega_{pk} \end{bmatrix}, {}^{B}\bar{\omega}_{B/I} = \begin{bmatrix} \omega_{Bn} \\ \omega_{Be} \\ \omega_{Bk} \end{bmatrix}, {}^{A}\bar{\omega}_{A/I} = \begin{bmatrix} \omega_{Ar} \\ \omega_{Ae} \\ \omega_{Ad} \end{bmatrix} \quad (2) $$

Where $\omega_{pi}, \omega_{pj}, \omega_{pk}$ are the body angular velocities of frame P in relation to inertial space about i, j, and k axes respectively, $\omega_{Be}, \omega_{Bn}, \omega_{Bk}$ are the azimuth gimbal angular velocities in relation to inertial space about n, e, and k axes respectively, and $\omega_{Ar}, \omega_{Ae}, \omega_{Ad}$ are the elevation gimbal angular velocities in relation to inertial space about the r, e, and d axes respectively. Inertia matrices of elevation and azimuth gimbals are

$$ {}^{A}J_{inner} = \begin{bmatrix} A_r & A_{re} & A_{rd} \\ A_{re} & A_e & A_{de} \\ A_{rd} & A_{de} & A_d \end{bmatrix}, \; {}^{B}J_{outer} = \begin{bmatrix} B_n & B_{ne} & B_{nk} \\ B_{ne} & B_e & B_{ke} \\ B_{nk} & B_{ke} & B_k \end{bmatrix} \quad (3) $$

Where A_r, A_e, A_d are elevation gimbal moments of inertia about r, e, and d axes, A_{re}, A_{rd}, A_{de} are elevation gimbal moments products of inertia, B_n, B_e, B_k are azimuth gimbal moments of inertia about n, e, and k axes, and B_{ne}, B_{nk}, B_{ke} are azimuth gimbal moments products of inertia. Also, it is introduced T_{EL} as the total external torque about the elevation gimbal e-axis, and T_{AZ} as the total external torque about the azimuth gimbal k-axis. As mentioned above, the aim is to stabilize the gimbal system LOS (r-axis) which means the angular velocities ω_{Ae} and ω_{Ad}, must be equal to zero. ω_{Ae}, ω_{Ad} can be measured by a rate gyro placed on the elevation gimbal. In general, Euler angles define the position between two related reference frames [21]. For the body fixed frame P and azimuth gimbal frame B with one angle η, these relations can be obtained

$$ \begin{aligned} \omega_{Bn} &= \omega_{Pi}\cos\eta + \omega_{Pj}\sin\eta \quad (a) \\ \omega_{Be} &= -\omega_{Pi}\sin\eta + \omega_{Pj}\cos\eta \quad (b) \\ \omega_{BK} &= \omega_{Pk} + \dot{\eta} \quad (c) \end{aligned} \quad (4) $$

Similarly, between azimuth gimbal frame B and elevation gimbal frame A we have

$$ \begin{aligned} \omega_{Ar} &= \omega_{Bn}\cos\varepsilon - \omega_{BK}\sin\varepsilon \quad (a) \\ \omega_{Ae} &= \omega_{Be} + \dot{\varepsilon} \quad (b) \\ \omega_{Ad} &= \omega_{Bn}\sin\varepsilon + \omega_{Bk}\cos\varepsilon \quad (c) \end{aligned} \quad (5) $$

The orientation of the gimbal system in an inertial system is completely determined by four independent consecutive rotations $\phi, \theta, \psi, \varepsilon$ where ϕ, θ, ψ are the three Euler rotations of the azimuth gimbal and ε is the elevation gimbal angle [5]. Then we can take these angles of rotations as the generalized coordinates in the Lagrange equations. The order of rotation is essential [5]. Fig.3 shows the order of consecutive Euler rotations of the azimuth gimbal.

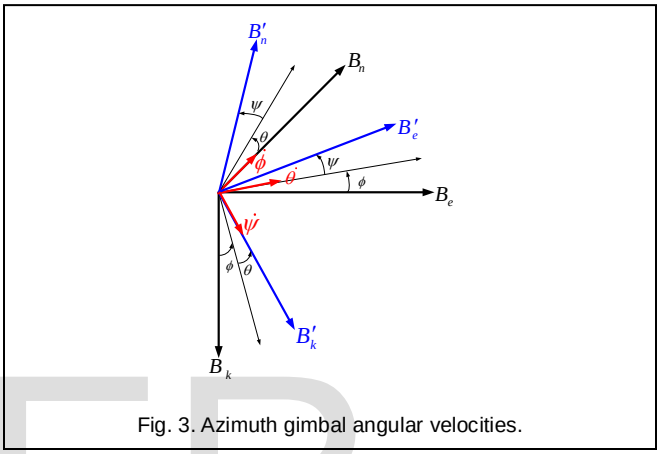

Fig. 3. Azimuth gimbal angular velocities.

By taking the rotations in the order roll(ϕ), elevation(θ), azimuth(ψ) followed by ε, the generalized "forces" corresponding to the coordinates ψ and ε are the external torques T_{AZ} and T_{EL} applied to the azimuth and elevation gimbals, respectively [5]. The kinetic energy of a rotating body is given by the scalar product [5].

$$ T = \bar{\omega} \cdot \frac{\bar{H}}{2} \; ; \; \bar{H} = J\bar{\omega} \quad (6) $$

Where $\bar{H}$ is the angular momentum, $\bar{\omega}$ is the inertial angular velocity of the body expressed in the body fixed frame, and J is the inertia matrix of the body. Thus the total kinetic energy of the two axes gimbal system is given by the sum of kinetic energy of elevation and azimuth gimbals.

$$ T = \bar{\omega} \cdot \frac{\bar{H}}{2}\bigg|_A + \bar{\omega} \cdot \frac{\bar{H}}{2}\bigg|_B \quad (7) $$

Inserting equations (2, 3) in (7) gives

$$ \begin{aligned} T = {} & \frac{1}{2}\left(A_r\omega_{Ar}^2 + A_e\omega_{Ae}^2 + A_d\omega_{Ad}^2\right) \\ & + \frac{1}{2}\left(B_n\omega_{Bn}^2 + B_e\omega_{Be}^2 + B_k\omega_{Bk}^2\right) \\ & + B_{ne}\omega_{Bn}\omega_{Be} + B_{nk}\omega_{Bn}\omega_{Bk} + B_{ke}\omega_{Be}\omega_{Bk} \\ & + A_{re}\omega_{Ar}\omega_{Ae} + A_{rd}\omega_{Ar}\omega_{Ad} + A_{de}\omega_{Ae}\omega_{Ad} \end{aligned} \quad (8) $$

Based on Fig.3 the azimuth gimbal angular velocities can be derived as follows

$$\omega_{Bn} = \dot{\phi}\cos\theta\cos\psi + \dot{\theta}\sin\psi$$
$$\omega_{Be} = -\dot{\phi}\cos\theta\sin\psi + \dot{\theta}\cos\psi \quad (9)$$
$$\omega_{Bk} = \dot{\phi}\sin\theta + \dot{\psi}$$

Using (9) and (5) in (8) give the kinetic energy as a function of the generalized coordinates and their time derivatives. Then, Lagrange equation can be formulated and equations of motion are obtained.

3.1 Azimuth Channel Relationships

The Lagrange equation for ψ is

$$\frac{d}{dt}\left(\frac{\partial T}{\partial \dot{\psi}}\right) - \frac{\partial T}{\partial \psi} = T_{AZ} \quad (10)$$

Where T is the kinetic energy given in (8) and T_{AZ} is the total external torque about the azimuth gimbal k-axis. As derived in Appendix A, the equation of azimuth gimbal motion can be derived as a differential equation for azimuth gimbal rate ω_{Bk}

$$J_{eq}\dot{\omega}_{Bk} = T_{Az} + T_{d1} + T_{d2} + T_{d3} \quad (11)$$

After some mathematical operations mentioned in appendix A, the equation (11) can be converted to the following form

$$J_{eq}\dot{\omega}_{Ad} = T_{Az}\cos\varepsilon + T_d\cos\varepsilon + T_d' \quad (12)$$

The complete derivation of azimuth channel relationships is illustrated in Appendix A.

3.2 Elevation Channel Relationships

Similarly, Lagrange equation for ε is

$$\frac{d}{dt}\left(\frac{\partial T}{\partial \dot{\varepsilon}}\right) - \frac{\partial T}{\partial \varepsilon} = T_{EL} \quad (13)$$

Where T_{EL} is the total external torque about the elevation gimbal e-axis. Then the elevation gimbal motion equation is obtained as a differential equation for the elevation rate ω_{Ae} in the following form

$$A_e\dot{\omega}_{Ae} = T_{EL} + (A_d - A_r)\omega_{Ar}\omega_{Ad} + A_{rd}(\omega_{Ar}^2 - \omega_{Ad}^2) - A_{de}(\dot{\omega}_{Ad} - \omega_{Ae}\omega_{Ar}) - A_{re}(\dot{\omega}_{Ar} + \omega_{Ae}\omega_{Ad}) \quad (14)$$

The complete derivation of elevation channel relationships is illustrated in Appendix B.

4 GIMBAL MASS UNBALNCE

4.1 Dynamic Mass unbalnce

The dynamic mass unbalance is the result of a non-symmetrical mass distribution called Product of Inertia (POI) [6]. The dynamic unbalance concept can be indicated by the inertia matrix. Therefore, if the considered gimbal has a symmetrical mass distribution with respect to its frame axes, then the gimbal has no dynamic unbalance and its inertia matrix is diagonal. On the other hand, if the gimbal has a non-symmetrical mass distribution with respect to its frame axes, then the gimbal has dynamic unbalance and its inertia matrix is not diagonal.

Actually, the same equations of motion for the azimuth gimbal (11) and elevation gimbal (14) have been obtained in [4], [5] using second Newton's law. However, these equations in [4], [5] were simplified assuming that the gimbals have no dynamic mass unbalance, which means that all products of inertia are zero $\left(A_{re} = A_{rd} = A_{de} = B_{ne} = B_{nk} = B_{ke} = 0\right)$. Therefore, the torque disturbance terms of elevation gimbal T_{D-EL} and azimuth gimbal T_{D-AZ} in [4], [5] were made less complex comparing to what has been carried out in this paper as it is clarified in Appendixes A and B.

4.2 Static Mass unbalnce

The static mass unbalance results from the offset between the pivot and the centre of gravity (CG). The applied acceleration reacts through the offset CG and produces a torque about the pivot (disturbance torque). Therefore, the actual LOS deviates from the desired LOS under acceleration forces. A correction torque (control torque) must be applied to prevent the gimbal deflection from its LOS [6]. Gimbal systems usually work in vibration environments which are characterized as a six degree of freedom (6 DOF); three of translational motion and three as angular motion. The angular degrees of freedom have little direct effect on the gimbal's reaction to a static unbalance; in this case, the mass properties driven response is mainly governed by inertia which serves to keep the gimbal pointed where it is. The modelled gimbal primarily responds to the three degrees of translational motion [6].

Ideally, the gimbal center of gravity (CG) is assumed to be precisely located at the pivot point. However, it is not always true in the actual hardware implementation. Thus, the CG location may displace from the pivot point [22]. In this paper, the disturbance torque due to static unbalance in elevation and azimuth gimbals is considered and obtained according to a reference frame XYZ on the assumption that the gimbal pivot is placed at the base CG point. For the elevation gimbal, the vertical plane XY just considered because the gimbal CG offset, which lies on the rotation axis, does not create any torque on the pivot as shown in Fig.4a. Therefore, Fig.4b indicates that the horizontal plane XZ is considered for the azimuth gimbal

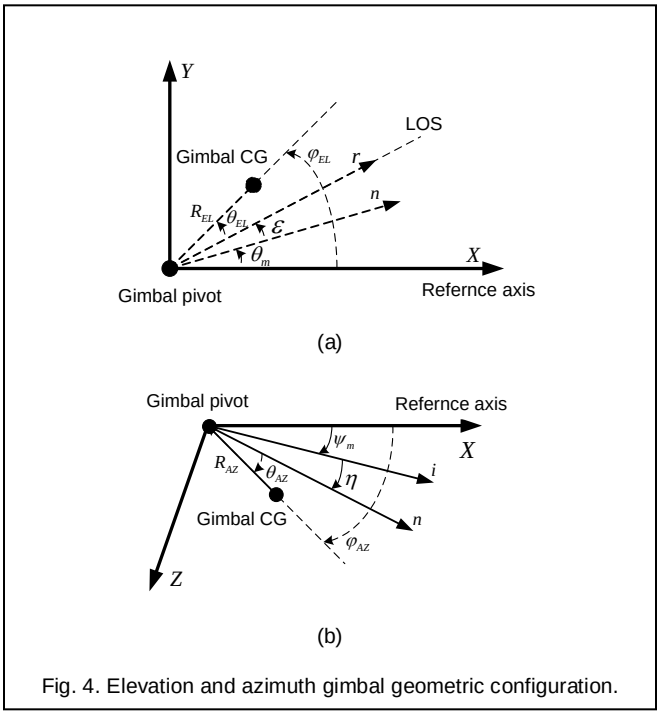

Fig. 4. Elevation and azimuth gimbal geometric configuration.

Based on what has been done in [22], the disturbance torques due to static unbalance in elevation and azimuth gimbals can be derived utilizing Euler equation for the variables φ_{EL} , φ_{AZ} as follows

$$T_{S-EL} = m_{EL} a_m R_{EL} \cos(\theta_m + \varepsilon + \theta_{EL})$$
$$T_{S-AZ} = m_{AZ} a_m R_{AZ} \cos(\psi_m + \eta + \theta_{AZ}) \quad (15)$$

Where, T_S is the disturbance torque due to static unbalance, a_m the affected lateral acceleration, θ_m the base body angle in vertical plane, ψ_m the base body angle in horizontal plane, m the mass of gimbal, R the gimbal offset distance, θ the gimbal offset angle, and EL, AZ are the index for elevation and azimuth gimbals respectively. It is worth mentioning that these disturbances disappear when the gimbal CG and gimbal pivot are exactly identical.

5 STABILIZATION LOOP CONSTRUCTION

In the following, the components of traditional stabilization loop indicated in Fig.2 will be identified. Although, the researchers tried to utilize and apply many different modern techniques to control inertia stabilization systems, the conventional PID and its constructors are often utilized because of its simplicity that makes it easy to be understood by the engineers [23] and implemented easily in the control process. Therefore, two PI controllers have been utilized (one for each channel)

$$K_{EL}(s) = 0.09 + \frac{12.5}{s} \quad , \quad K_{AZ}(s) = 0.5 + \frac{12.5}{s} \quad (16)$$

Any servo motion control system should have an actuator module that makes the system to actually perform its function. The most common actuator used to perform this task is the DC servomotor. DC motor is one of the simplest motor types. It is widely preferred for high performance systems requiring minimum torque ripple, rapid dynamic torque, speed responses, high efficiency and good inertia [24]. These motors speedily respond to a command signal by means of a suitable controller. In this kind of motors, the speed control is carried out by changing the supply voltage of the motor [25]. The DC motor can be expressed in a block digram shown in Fig.5

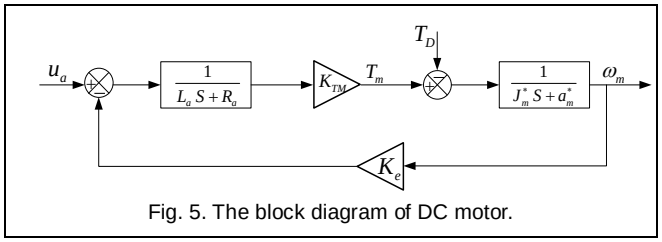

Fig. 5. The block diagram of DC motor.

DC motor from NORTHROP GRUMMAN Company (Table 1) is utilized in this paper. The transfer function of the DC motor can be obtained as follows

$$G_m(s) = \frac{\omega_m(s)}{u_a(s)} = \frac{K_{TM}}{(L_a s + R_a)\cdot(J_m^* s + a_m^*) + K_e K_{TM}} \quad (17)$$
$$= \frac{24637.68}{s^2 + 1500 s + 20942} \quad ; \quad a_m^* = 0$$

TABLE 1
DC MOTOR SPECIFICATIONS

Parameter	Value
Nominal voltage u_a	27 V
No load speed ω_{nl}	303 rpm
Terminal resistance R_a	4.5 Ω
Terminal inductance L_a	0.003 H
Torque constant K_{TM}	0.85 Nm/A
Back EMF K_e	0.85 V/rad/sec
Rotor inertia J_m	0.0017 Kgm^2
Damping ratio a_m	0

Where ω_m is the motor's angular velocity, u_a the motor's armature voltage, T_m the torque generated by the motor, T_D the torque disturbance. Also, $J_m^* = J_m + J_L$ and $a_m^* = a_m + a_L$ where J_L is the platform's moment of inertia, a_L is the load's damping ratio. The platform (or what can be named the inertia) represents the motor load, which is attached to the output of the gears or directly to the shaft motor.

The platform is modelled based on its moment of inertia J_L that depends on its dimensions and its position respect to the axis of rotation. In this paper, a discus is proposed to represent the platform where its mass $M = 1kg$ and radius $r = 14cm$, so $J_L = 9.8\times10^{-3} Kg.m^2$.

In this paper, the 475T rate gyroscope from the US Dynamics company is considered. Table 2 indicates this gyro specification.

TABLE 2
GYROSCOPE CHARACTERISTICS

Input Rate	From ± 40 to ±1000 °/sec
output	AC or DC
Scale Factor	Customer Specification
Natural Frequency	20 to 140 Hz
Damping Ratio	0.4 to 1.0

The rate gyro can be modelled in the second order system typically [26]. For the gyro of natural frequency $\omega_n = 50\,Hz$ and the damping ratio $\zeta = 0.7$, the gyro transfer function is

$$G_{Gyro}(s) = \frac{\omega_n^2}{(s^2 + 2\zeta\omega_n s + \omega_n^2)} = \frac{2500}{(s^2 + 70s + 2500)} \quad (18)$$

If gimbal design is not proper, the control algorithms may become complex and it may not be possible to meet the performance criteria [27]. While the well-designed gimbal assem-

bly reduces the jitter of sensor's line of sight and hence needs a simpler control system [3], [27] which simplifies the implementation of control laws in real time. As mentioned above, the drawback of the traditional stabilization loop appears when the control system work under variable conditions. Therefore, the cascade control technique is proposed. The traditional stabilization loop can be converted into cascade one by adding the following PI controller as shown in Fig.6.

$$G_{PI}(s) = 40 + \frac{5}{s} \quad (19)$$

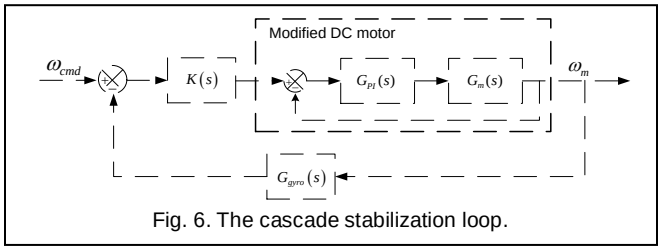

Fig. 6. The cascade stabilization loop.

Where ω_{cmd} is the input rate command. The added PI controller and DC motor constitute the inner feedback loop or sub-block entitled modified DC motor.

6 SIMULATION AND RESULTS

Based on the gimbals mathematical model obtained above, the proposed cascade stabilization loop, and by taking into account the dynamic and static mass unbalance, the overall control system of the two axes gimbal system is constructed and simulated in MATLAB/Simulink environment as indicated in Fig.7.

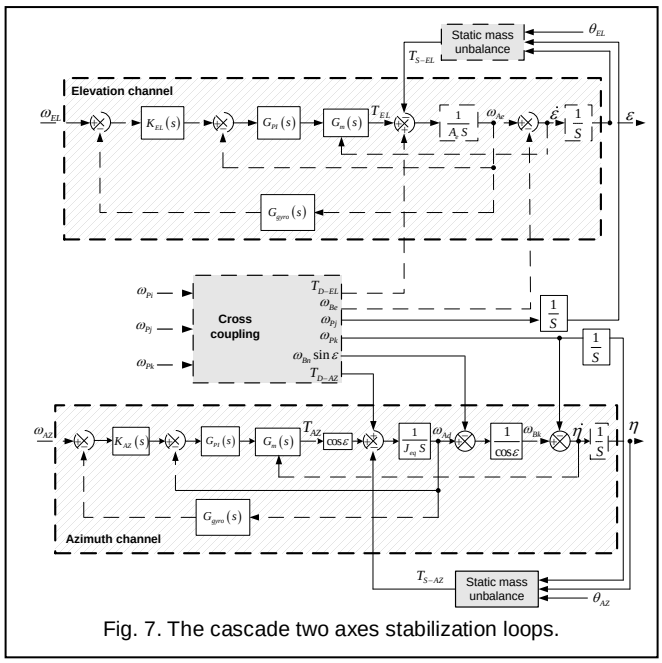

Fig. 7. The cascade two axes stabilization loops.

In order to take the effect of base angular motion into account, the rates $\dot{\varepsilon}, \dot{\eta}$ must be fed back to the DC motors of elevation and azimuth channels respectively through the motor electrical constant (back emf constant).

Two tests will be made to carry out a comparison between the traditional and cascade stabilization loop in order to investigate the effects of the base rate and acceleration change on the performance of two axes gimbal system.

6.1 Test 1: Base Rate Change

This test is made according to many diffirent scenarios indicated in Table 3 assuming that there is no acceleration applied on the gimbal system and for input rate commands $\omega_{EL} = \omega_{AZ} = 10$ deg/sec in elevation and azimuth channels respectively.

TABLE 3
TEST 1 SCENARIOS

scenario	Base angular velocities (deg/sec)		
	ω_{Pi}	ω_{Pj}	ω_{Pk}
S1	0	0	0
S2	5	5	5
S3	10	10	10
S4	15	15	15

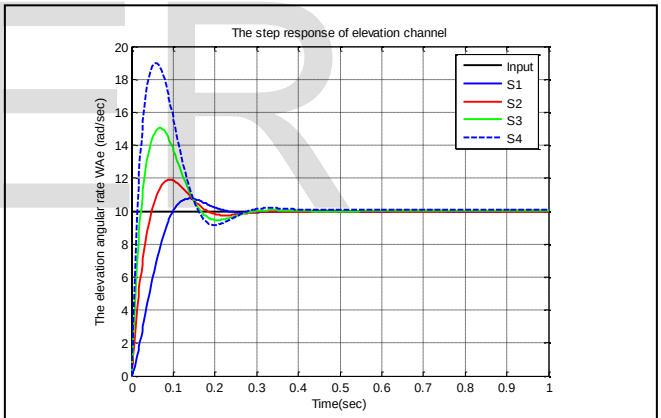

(a) traditional loop

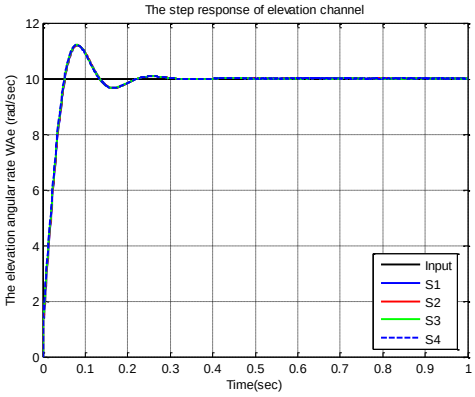

(b) cascade loop

Fig. 8. The elevation loop response for differenet rates.

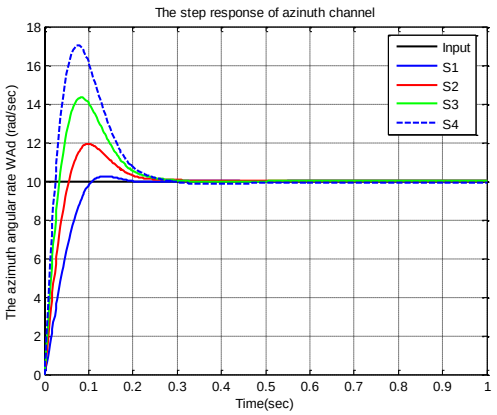

(a) traditional loop

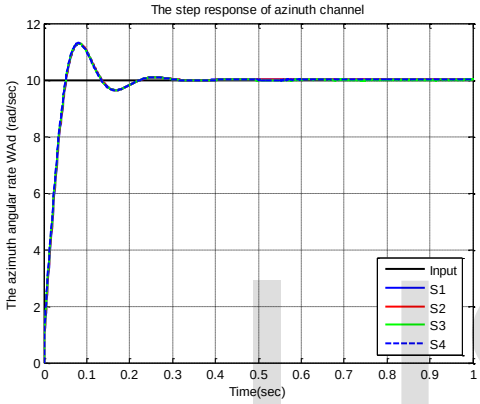

(b) cascade loop

Fig. 9. The azimuth loop response for different rates.

The tests results shown in Fig.8 and Fig.9 indicate that when the traditional control is used the response overshoot of elevation and azimuth channels increase as well as a steady state error appears and increases more and more whenever the base rate increases. On the other hand, it is realized that the cascade stabilization loop improves the performance of both channels by maintaining good response with fixed acceptable overshoot and without any steady state error.

6.2 Test 2: Base Acceleration Change

Equations 15 show that the torque disturbances due to static mass unbalance increase sharply when the base acceleration increase. Therefore, the overall control system shown in Fig.7 is tested for many diffirent accelerations assuming that the base angular velocitie are fixed. All the acceleration and rate values as well as other parameters considered in test2 are indicated in Table 4.

TABLE 4
TEST 2 PARAMETERS

Base rates (deg/sec)	$\omega_{p_i} = 5, \omega_{p_j} = 10, \omega_{p_k} = 15$
Accelerations (g)	$a_{m1} = 100, a_{m2} = 200, a_{m3} = 300, a_{m4} = 400$
Offset distances (deg)	$R_{EL} = R_{AZ} = 0.00076$
Offset angles (m)	$\theta_{EL} = \theta_{AZ} = 0.0001$

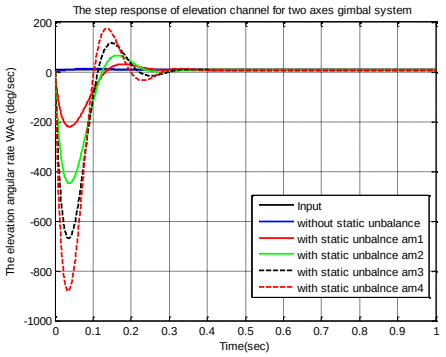

(a) traditional loop

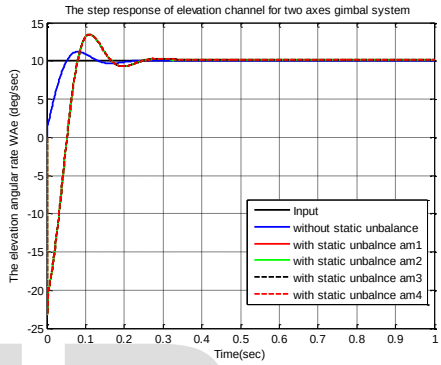

(b) cascade loop

Fig. 10. The elevation loop response for different accelerations.

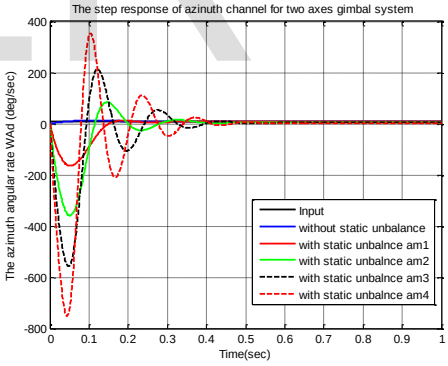

(a) traditional loop

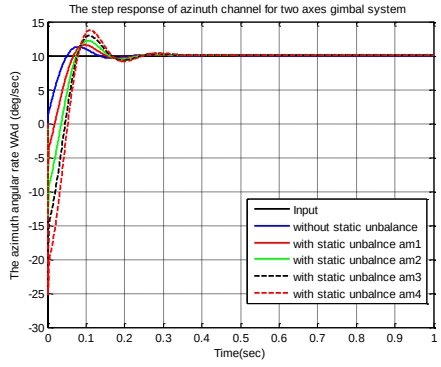

(b) cascade loop

Fig. 11. The azimuth loop response for different accelerations.

Fig.10 and Fig.11 show the effects of base acceleration change on the performance of gimbal system for traditional and cascade loops in both elevation and azimuth channels respectively. It is clear that utilizing the cascade stabilization loop causes a large improvement in the transient and steady state response for elevation and azimuth channels. The cascade technique can dramatically reduce the overshoot and settling time in addition to eliminating the steady state error.

It is important to test the performance of the cascade control technique when it is used to build the tracking system that works under variable accelerations. The tracking loop can be built as a closed feedback loop which includes the stabilization loop. For example, the construction of elevation tracking loop is displayed in Fig.12 where the stabilization loop is replaced by its equivalent closed loop transfer function $G_{stab}(s)$.

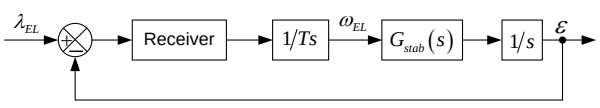

Fig. 12. The elevation tracking loop.

The angle channel receiver may have unity transfer function and measures the pointing error between the output ε and the input LOS angle λ_{EL}. The time constant of the tracking loop T considered equals to 0.08 sec. Utilizing the structure in Fig.12, the simulink model of gimbal system shown in Fig.7 is developed into tracking system then test 2 is applied.

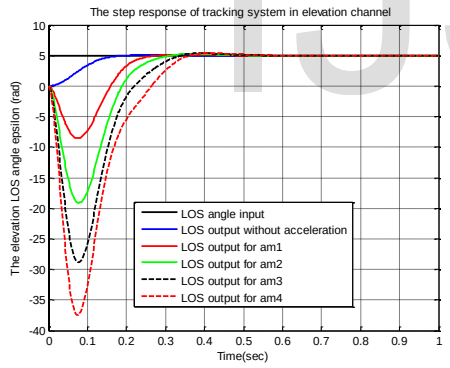

(a) traditional loop

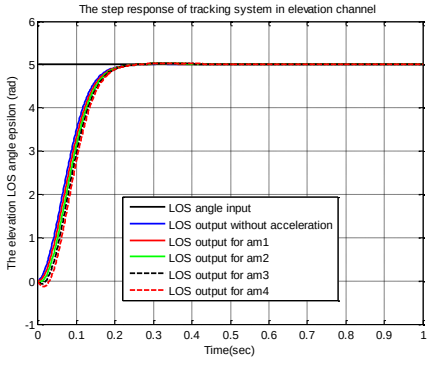

(b) cascade loop

Fig. 13. The elevation tracking loop response for different accelerations.

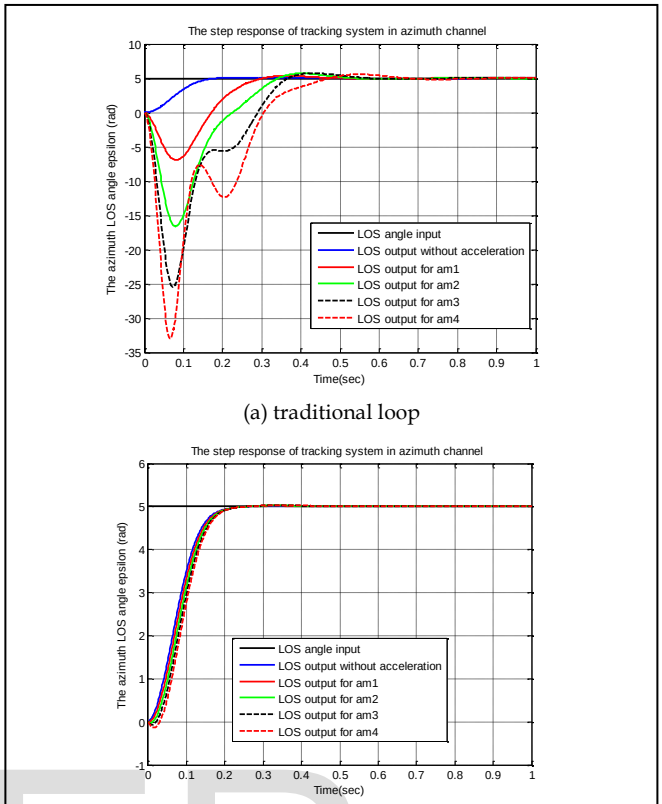

(a) traditional loop

(b) cascade loop

Fig. 14. The azimuth tracking loop response for different accelerations.

Fig.13 and Fig.14 confirm that the cascade approach is very effective in improving the performance of tracking system against the base acceleration change especially the transient response which can be achieved in less settling time with zero overshoot comparing with traditional loop. Also, the steady state response is achieved using cascade technique with zero steady state error.

7 CONCLUSION

In this paper, the two axes gimbal system has been introduced. The gimbals mathematical model has been derived using Lagrange equation. The complete gimbal system has been constructed by taking into account the base angular rates, the mass unbalance, and the cross coupling between elevation and azimuth channels. The gimbal system created in MATLAB/Simulink has been tested under variable rates and accelerations using both traditional and proposed cascade control techniques. The results obtained have ensured the efficiency of proposed cascade control which has offered better performance compared with the traditional control. The cascade control has highly improved the transient and steady state response of the two axes gimbal stabilization system against the variable rates and accelerations. Also, when the cascade control has been used, the performance of two axes gimbal tracking system has been dramatically enhanced against the base acceleration change.

Appendix A (Azimuth channel)

Utilizing (9) gives

$$\frac{\partial \omega_{Bn}}{\partial \dot{\psi}} = 0 \ , \ \frac{\partial \omega_{Be}}{\partial \dot{\psi}} = 0 \ , \ \frac{\partial \omega_{Bk}}{\partial \dot{\psi}} = 1$$
$$\frac{\partial \omega_{Bn}}{\partial \psi} = \omega_{Be} \ , \ \frac{\partial \omega_{Be}}{\partial \psi} = -\omega_{Bn} \ , \ \frac{\partial \omega_{Bk}}{\partial \psi} = 0 \qquad (A.1)$$

Then from (5) and (9) we have

$$\frac{\partial \omega_{Ar}}{\partial \dot{\psi}} = -\sin\varepsilon \ , \ \frac{\partial \omega_{Ae}}{\partial \dot{\psi}} = 0 \ , \ \frac{\partial \omega_{Ad}}{\partial \dot{\psi}} = \cos\varepsilon$$
$$\frac{\partial \omega_{Ar}}{\partial \psi} = \omega_{Be}\cos\varepsilon \ , \ \frac{\partial \omega_{Ae}}{\partial \psi} = -\omega_{Bn} \ , \ \frac{\partial \omega_{Ad}}{\partial \psi} = \omega_{Be}\sin\varepsilon \qquad (A.2)$$

Using (A.1) and (A.2), the two terms in the left side of (10) are converted into

$$\frac{\partial T}{\partial \dot{\psi}} = -\left(A_r\omega_{Ar} + A_{re}\omega_{Ae} + A_{rd}\omega_{Ad}\right)\sin\varepsilon + \left(A_{rd}\omega_{Ar} + A_{de}\omega_{Ae} + A_d\omega_{Ad}\right)\cos\varepsilon + B_{nk}\omega_{Bn} + B_{ke}\omega_{Be} + B_k\omega_{Bk} \qquad (A.3)$$

$$\frac{\partial T}{\partial \psi} = -\omega_{Bn}\left(B_{ne}\omega_{Bn} + B_e\omega_{Be} + B_{ke}\omega_{Bk} + A_{re}\omega_{Ar} + A_e\omega_{Ae} + A_{de}\omega_{Ad}\right) + \omega_{Be}\left(B_n\omega_{Bn} + B_{ne}\omega_{Be} + B_{nk}\omega_{Bk}\right) + \omega_{Be}\left(A_r\omega_{Ar} + A_{re}\omega_{Ae} + A_{rd}\omega_{Ad}\right)\cos\varepsilon + \omega_{Be}\left(A_{rd}\omega_{Ar} + A_{de}\omega_{Ae} + A_d\omega_{Ad}\right)\sin\varepsilon \qquad (A.4)$$

Based on (A.3), (A.4), and (5) the equation of azimuth gimbal motion can be derived as a differential equation for azimuth gimbal rate ω_{Bk}.

$$J_{eq}\dot{\omega}_{Bk} = T_{Az} + T_{d1} + T_{d2} + T_{d3} \qquad (A.5)$$

Where. $T_d = T_{d1} + T_{d2} + T_{d3}$. represents different azimuth gimbal inertia disturbances, J_{eq} is the instantaneous moment of inertia about the k-axis. All components are defined as follows

$$J_{eq} = B_k + A_r\sin^2\varepsilon + A_d\cos^2\varepsilon - A_{rd}\sin(2\varepsilon) \qquad (A.6)$$

$$T_{d1} = \begin{bmatrix} B_n + A_r\cos^2\varepsilon + A_d\sin^2\varepsilon \\ +A_{rd}\sin(2\varepsilon) - (B_e + A_e) \end{bmatrix}\omega_{Bn}\omega_{Be} \qquad (A.7)$$

$$T_{d2} = -(B_{ke} + A_{de}\cos\varepsilon - A_{re}\sin\varepsilon)(\dot{\omega}_{Be} + \omega_{Bn}\omega_{Bk}) - (B_{ne} + A_{re}\cos\varepsilon + A_{de}\sin\varepsilon)(\omega_{Bn}^2 - \omega_{Be}^2) - \left[B_{nk} + (A_d - A_r)\sin\varepsilon\cos\varepsilon + A_{rd}\cos(2\varepsilon)\right](\dot{\omega}_{Bn} - \omega_{Be}\omega_{Bk}) \qquad (A.8)$$

$$T_{d3} = \dot{\varepsilon}\left[(A_r - A_d)(\omega_{Bn}\cos(2\varepsilon) - \omega_{Bk}\sin(2\varepsilon))\right] + \dot{\varepsilon}\left[2A_{re}(\omega_{Bn}\sin(2\varepsilon) + \omega_{Bk}\cos(2\varepsilon))\right] + \ddot{\varepsilon}(A_{re}\sin\varepsilon - A_{de}\cos\varepsilon) + \dot{\varepsilon}\left[(A_{de}\sin\varepsilon + A_{re}\cos\varepsilon)(\omega_{Ae} + \omega_{Be}) - A_e\omega_{Bn}\right] \qquad (A.9)$$

Inserting $\dot{\omega}_{Bk}$ obtained from (5c) in (A.5) converts it into a differential equation for the elevation rate ω_{Ad} as follows

$$J_{eq}\dot{\omega}_{Ad} = T_{Az}\cos\varepsilon + T_d\cos\varepsilon + T_d' \quad ; \quad T_d' = J_{eq}\left[\dot{\omega}_{Bn}\sin\varepsilon + \omega_{Ar}\left(\omega_{Ae} - \omega_{Be}\right)\right] \qquad (A.10)$$

The disturbances affected on azimuth gimbal are denoted by

$$T_{D-AZ} = \left(T_{d1} + T_{d2} + T_{d3}\right)\cos\varepsilon + T_d' \qquad (A.11)$$

The term T_{d1} well be denoted as T_{D-AZ1}. Then, using $\dot{\omega}_{Bn}$ from (4a), ω_{Bk} from (5c), $\dot{\omega}_{Be}$ from (4b), and (5b) the terms T_{d2} and T_{d3} are modified into T_{D-AZ2} and T_{D-AZ3} respectively.

$$T_{D-AZ2} = \left[B_{nk} + (A_d - A_r)\sin\varepsilon\cos\varepsilon + A_{rd}(2\cos^2\varepsilon - 1)\right] \times\left(-\dot{\omega}_{p_j}\sin\eta - \dot{\omega}_{p_i}\cos\eta + \omega_{Be}\omega_{p_k}\right) - (B_{ke} + A_{de}\cos\varepsilon - A_{re}\sin\varepsilon)\left(\dot{\omega}_{p_j}\cos\eta - \dot{\omega}_{p_i}\sin\eta + \omega_{Bn}\omega_{p_k}\right) - (B_{ne} + A_{re}\cos\varepsilon + A_{de}\sin\varepsilon)(\omega_{Bn}^2 - \omega_{Be}^2) \qquad (A.12)$$

$$T_{D-AZ3} = \dot{\omega}_{Ae}(A_{re}\sin\varepsilon - A_{de}\cos\varepsilon) + \omega_{Ad}\omega_{Bn}\left(A_{de} - A_{re}tg\varepsilon\right) + (A_{de}\cos\varepsilon - A_{re}\sin\varepsilon)\left(\dot{\omega}_{p_j}\cos\eta - \dot{\omega}_{p_i}\sin\eta\right) + \omega_{Bn}^2\left(A_{re}tg\varepsilon - A_{de}\right)\sin\varepsilon + 2\omega_{Ad}\omega_{Be}(A_r - A_d)\sin\varepsilon + 2A_{re}\omega_{Ad}(\omega_{Ae} - \omega_{Be})\left(2\cos\varepsilon - \frac{1}{\cos\varepsilon}\right) + \left(\omega_{Ae} - \omega_{Be}\right)\left[(A_{de}\sin\varepsilon + A_{re}\cos\varepsilon)\left(\omega_{Ae} + \omega_{Be}\right) - A_e\omega_{Bn}\right] + 2A_{re}\left(\omega_{Ae} - \omega_{Be}\right)\omega_{Bn}tg\varepsilon + \omega_{Ae}\omega_{Bn}(A_r - A_d) \qquad (A.13)$$

From (5a) we have

$$\omega_{Ar} = -\omega_{Ad}tg\varepsilon + \frac{\omega_{Bn}}{\cos\varepsilon} \qquad (A.14)$$

Using ω_{Bk} from (5c), $\dot{\omega}_{Bn}$ from (4a), and ω_{Ar} from (A.14), the term T_d' becomes

$$T_{D-AZ4} = J_{eq}[-\omega_{Be}\omega_{Bn}\left(\frac{1+\sin^2\varepsilon}{\cos\varepsilon}\right) - \omega_{Ad}\omega_{Ae}tg\varepsilon + 2\omega_{Ad}\omega_{Be}tg\varepsilon + \left(\dot{\omega}_{p_i}\cos\eta + \dot{\omega}_{p_j}\sin\eta\right)\sin\varepsilon - \omega_{Be}\omega_{p_k}\sin\varepsilon + \frac{\omega_{Ae}\omega_{Bn}}{\cos\varepsilon}] \qquad (A.15)$$

Appendix B (Elevation channel)

The kinetic energy for elevation gimbal is

$$T = \left(\bar{\omega}\cdot\frac{\bar{H}}{2}\right)_A = \frac{1}{2}\left(A_r\omega_{Ar}^2 + A_e\omega_{Ae}^2 + A_d\omega_{Ad}^2\right) + A_{re}\omega_{Ar}\omega_{Ae} + A_{rd}\omega_{Ar}\omega_{Ad} + A_{de}\omega_{Ae}\omega_{Ad} \qquad (B.1)$$

From (5) we have

$$\frac{\partial \omega_{Ar}}{\partial \dot{\varepsilon}} = 0 \ , \ \frac{\partial \omega_{Ae}}{\partial \dot{\varepsilon}} = 1 \ , \ \frac{\partial \omega_{Ad}}{\partial \dot{\varepsilon}} = 0$$
$$\frac{\partial \omega_{Ar}}{\partial \varepsilon} = -\omega_{Ad} \ , \ \frac{\partial \omega_{Ae}}{\partial \varepsilon} = 0 \ , \ \frac{\partial \omega_{Ad}}{\partial \varepsilon} = \omega_{Ar} \qquad (B.2)$$

$$\frac{\partial T}{\partial \varepsilon} = \omega_{Ar}\omega_{Ad}\left(A_d - A_r\right) - A_{re}\omega_{Ad}\omega_{Ae} - A_{rd}\left(\omega_{Ar}^2 - \omega_{Ad}^2\right) + A_{de}\omega_{Ar}\omega_{Ae} \qquad (B.3)$$

$$\frac{\partial T}{\partial \dot{\varepsilon}} = A_e\omega_{Ae} + A_{re}\omega_{Ar} + A_{de}\omega_{Ad}$$

Using (B-3) in (13) gives the elevation gimbal motion equation as a differential equation for the elevation angular velocity ω_{Ae} as follows

$$A_e\dot{\omega}_{Ae} = T_{EL} + (A_d - A_r)\omega_{Ar}\omega_{Ad} + A_{rd}(\omega_{Ar}^2 - \omega_{Ad}^2) - A_{de}(\dot{\omega}_{Ad} - \omega_{Ae}\omega_{Ar}) - A_{re}(\dot{\omega}_{Ar} + \omega_{Ae}\omega_{Ad}) \qquad (B.4)$$

It can be seen that the elements of inertia matrix form the disturbance term T_{D-EL}.

$$T_{D-EL} = (A_d - A_r)\omega_{Ar}\omega_{Ad} + A_{rd}(\omega_{Ar}^2 - \omega_{Ad}^2) - A_{de}(\dot{\omega}_{Ad} - \omega_{Ae}\omega_{Ar}) - A_{re}(\dot{\omega}_{Ar} + \omega_{Ae}\omega_{Ad}) \qquad (B.5)$$

Using $\dot{\omega}_{Bn}$ from (4a), $\dot{\omega}_{Bk}$ from (5c), and (5) converts the disturbance term (B.5) as follows

$$T_{D-EL} = T_{D-EL1} + T_{D-EL2} .... + T_{D-EL10} \quad \text{(B.6)}$$

$$T_{D-EL1} = \left(A_{de}\sin\varepsilon + A_{re}\cos\varepsilon\right)\begin{bmatrix} \dfrac{-2\omega_{Be}\omega_{Ad} - 2\omega_{Be}\omega_{Bn}\sin\varepsilon}{\cos\varepsilon} \\ +\omega_{Be}\omega_{p_k} - \dot{\omega}_{p_i}\cos\eta + \dot{\omega}_{p_j}\sin\eta \end{bmatrix} \quad \text{(B.7)}$$

$$T_{D-EL2} = \omega_{Be}\omega_{Bn}\left(A_{de}\cos\varepsilon - A_{re}\sin\varepsilon\right) \quad \text{(B.8)}$$

$$T_{D-EL3} = \left(A_d - A_r\right)\left[2\cos\varepsilon - \frac{1}{\cos\varepsilon}\right]\left[\omega_{Bn}\omega_{Ad} - \omega^2{}_{Bn}\sin\varepsilon\right] \quad \text{(B.9)}$$

$$T_{D-EL4} = -4A_{rd}\omega_{Bn}\omega_{Ad}\sin\varepsilon \quad \text{(B.10)}$$

$$T_{D-EL5} = 2A_{rd}\omega_{Bn}\omega_{Ad}tg^2\varepsilon \quad \text{(B.11)}$$

$$T_{D-EL6} = A_{rd}\omega^2{}_{Ad}\left[\frac{1}{\cos^2\varepsilon} - 2\right] \quad \text{(B.12)}$$

$$T_{D-EL7} = \left(\dot{\omega}_{p_k} + \ddot{\eta}\right)\left[A_{re}\sin\varepsilon - A_{de}\cos\varepsilon\right] \quad \text{(B.13)}$$

$$T_{D-EL8} = A_{rd}\omega^2_{Bn}\left[-2\sin^2\varepsilon + tg^2\varepsilon\right] \quad \text{(B.14)}$$

$$T_{D-EL9} = \left(A_d - A_r\right)\sin\varepsilon\cos\varepsilon + 2A_{rd}\omega^2_{Bn} \quad \text{(B.15)}$$

$$T_{D-EL10} = \left(A_d - A_r\right)tg\varepsilon\begin{bmatrix} 2\omega_{Ad}\omega_{Bn}\sin\varepsilon \\ -\omega^2_{Ad} - \omega^2_{Bn}\sin^2\varepsilon \end{bmatrix} \quad \text{(B.16)}$$

REFERENCES

[1] M.K. Masten, "Inertially Stabilized Platform for Optical Imaging Systems", IEEE *Control Systems Magazine*, vol 28, pp. 47-64, 2008.

[2] S. C. Rybak, "Analytic Study of inside-out / coincident gimbal dynamics", *Final report, The Bendix corporation, Guidance System divison*, vol. 1, 1976.

[3] L.A. Stokum and G.R. Carroll, "Precision stabilized platform for shipborne electro-optical systems", *SPIE*, vol. 493, pp. 414-425, 1984.

[4] A.K. Rue, "precision stabilization systems", IEEE *Trans. Aerospace and Electronic Systems*, AES-10, pp. 34-42, 1974.

[5] B. Ekstrand, "Equation of Motion for a Two Axes Gimbal System", IEEE *Trans. On Aerospace and Electronic Systems*, vol. 37, pp. 1083-1091, 2001.

[6] R. Daniel, "Mass properties factors in achieving stable imagery from a gimbal mounted camera", *Published in SPIE Airborne Intelligence, Surveillance, Reconnaissance (ISR) Systems and Applications* V. 6946, 2008.

[7] H. Özgür, E. Aydan, and E. İsmet, "Proxy-Based Sliding Mode Stabilization of a Two-Axis Gimbaled Platform", *Proceedings of the World Congress on Engineering and Computer Science* (WCECS), San Francisco. USA, vol. I, 2011.

[8] S. Ravindra, "Modeling and Simulation of the Dynamics of a Large Size Stabilized Gimbal Platform Assembly", *Asian International Journal of Science and Technology in Production and Manufacturing*, vol. 1, pp. 111-119, 2008.

[9] H. Khodadadi, "Robust control and modeling a 2-DOF Inertial Stabilized Platform", *International Conference on Electrical, Control and Computer Engineering*, Pahang, Malaysia, 2011.

[10] B.J. Smith, W.J. Schrenck, W.B Gass, and Y.B. Shtessel, "Sliding mode control in a two axis gimbal system", *in Proc.* IEEE *Aerospace Applicat. Conf*, vol. 5, pp. 457–470, 1999.

[11] J.B. Willian, and P.T. Steven, "Optimal motion stabilization control of an electrooptical sight system", *Proc. SPIE Conference*, vol. 1111, pp. 116–120, 1989.

[12] L. Bo, D. Hullender, and M. DeRenzo, "Nonlinear induced disturbance rejection in inertial stabilization systems", IEEE *Trans,* vol. 6, pp. 421–427, 1998.

[13] J.A.R. Krishna Moorty, R. Marathe, and B. Hari, "Fuzzy controller for line of sight stabilization system", *Optical Engineering*, vol. 43, pp. 1394–1400, 2004.

[14] C.M. Lin, C.F. Hsu, and Y.J Mon, "Self-organizing fuzzy learning CLOS guidance law design", IEEE *Trans*, AES. 39, pp. 1144–1151, 2003.

[15] K.K. Tam, T.H. Lee, A. Mamum, M.W. Lee, and C.J. Khoh, "composite control of a gyro mirror line of sight stabilization platform design and auto tuning", *ISA transaction*, vol. 40, pp. 155-171, 2001.

[16] J.A.R. Krishna Moorty, R. Marathe, and V.R. Sule, "H∞ control law for line-ofsight stabilization for mobile land vehicles", *Optical Engineering*, vol. 41, pp. 2935–2944, 2002.

[17] K.C. Tan, T.H. Lee, and E.F. Khor, "Design and real-time implementation of a multivariable gyro-mirror line-of-sight stabilization platform", *Fuzzy Sets and Systems*, vol. 128, pp. 81–93, 2002.

[18] K.Z. Tang, S.N. Huang, K.K. Tan, and T.H. Lee, "Combined PID and adaptive nonlinear control for servo mechanical systems", *Mechatronics*, vol. 14, pp. 701-714, 2004.

[19] M.F. Rahmat, Sy. Najib, and Sy. Salim, "Non-linear Modeling and Cascade Control of an Industrial Pneumatic Actuator System", *Australian Journal of Basic and Applied Sciences*, pp. 465-477, 2011.

[20] P.J. Kennedy, and R.L. Kennedy, "Direct versus indirect line of sight (LOS) stabilization", IEEE *Transactions on Control Systems Technology*, vol. 11, pp. 3-15, 2003.

[21] S. Yu, and Y. Zhao, "A New Measurement Method for Unbalanced Moments in a two-axis Gimbaled Seeker", *Chinese Journal of Aeronautics*, vol. 23, pp. 117-122, 2010.

[22] L. Chun, and H. Yi, "Adaptive Feedforward Control for Disturbance Torque Rejection in Seeker Stabilizing Loop", IEEE *Transactions On Control Systems Technology*, vol. 9, no. 1, pp. 108-121, 2001.

[23] K. Tang, S. Huang, K. Tan, and T. Lee, "Combined PID and adaptive nonlinear control for servo mechanical systems", *Mechatronics*, vol. 14, pp.701-714, 2004.

[24] R. Malhotra, N. Singh, and Y. Singh, "Design of Embedded Hybrid Fuzzy-GA Control Strategy for Speed Control of DC Motor: A Servo Control Case Study", *International Journal of Computer Applications*, vol. 6, pp. 37-46, 2010.

[25] H. Fujita, and J. Sasaki, "Torque Control for DC Servo Motor using Adaptive Load Torque Compensation", *Proceedings of the 9thWSEAS international conference on System science and simulation in engineering*, pp. 454-458, 2010.

[26] L. Ho-Pyeong, and Y. Inn-Eark, "Robust Control Design for a Two-axis Gimbaled Stabilization System", IEEEAC paper #1010, Version 3, 2007.

[27] M.K. Masten, and J.M Hilkert, "Electromechanical system configuration for pointing, tracking and stabilization application", *SPIE*, vol. 779, pp. 75-87, 1987.